



# Numerical simulation of resistance furnaces by using distributed and lumped models

A. Bermúdez<sup>1,2</sup> · D. Gómez<sup>1,2</sup> · D. González<sup>1</sup>

Received: 3 October 2023 / Accepted: 26 February 2024 / Published online: 10 April 2024  
© The Author(s) 2024

## Abstract

This work proposes a methodology that combines distributed and lumped models to simulate the current distribution within an indirect heat resistance furnace and, in particular, to calculate the current to be supplied for achieving a desired power output. The distributed model is a time-harmonic eddy current problem, which is solved numerically using the finite element method. The lumped model relies on calculating a reduced impedance associated with an equivalent circuit model. Numerical simulations and plant measurements demonstrate the effectiveness of this approach. The good correlation between the results indicates that this approximation is well-suited to support the design and improve the efficiency of the furnace in a short time.

**Keywords** Metallurgical furnaces · Indirect resistance heating · Equivalent circuit model · AC impedance · Active power estimation

**Mathematics Subject Classification (2010)** 35Q61 · 65N30 · 68Q06

---

Communicated by: Francesca Rapetti

---

This article is dedicated to Professor Alain Bossavit on the occasion of his 80th birthday.

---

✉ A. Bermúdez  
alfredo.bermudez@usc.es

D. Gómez  
mdolores.gomez@usc.es

D. González  
david.gonzalez.penas@rai.usc.es

<sup>1</sup> Department of Applied Mathematics, Universidade de Santiago de Compostela, E-15782 Santiago de Compostela, Spain

<sup>2</sup> Galician Centre for Mathematical Research and Technology (CITMAga), E-15782 Santiago de Compostela, Spain

## 1 Introduction

Numerical simulation is now a tool of paramount importance for engineering design. This is particularly true in the field of electromagnetism, where the contribution of Alain Bossavit has been fundamental in the introduction and analysis of numerical methods for solving Maxwell's equations (see, for instance, among his numerous publications, the reference book [8]). The present paper deals with a good example of the engineering application of this methodology to simulate the behavior of a resistance furnace.

In the last years, indirect resistance heating has found an increasing application in different manufacturing processes, particularly in the metallurgical, ceramic, electronic, glass, and semiconductor industries ([14, 27]). In metallurgy, one of the main advantages is that it allows the energy to be distributed uniformly over the workpiece, which is essential for certain industrial processes.

This paper focuses on electric indirect heat resistance furnaces used for metal purification. In these devices, heating essentially occurs because the current supplied to the furnace passes through the resistance, where electric energy is transformed into thermal energy. The heat is then transferred to the load by radiation, convection, and/or conduction. For furnaces operating at high temperatures, radiation is the primary mode of heat transfer. Typically, alternating current is used, and some heat is also generated, but to a much lesser extent, due to the Joule effect resulting from the eddy currents induced in the conducting parts of the domain.

This is an energy-intensive industrial process and considerable efforts are being made to optimize its operation. In general, resistance heating is used when demand patterns are not suitable for induction furnaces and therefore cannot be considered as a competitive technique [1]. For instance, in metal melting processes, resistance furnaces offer the advantage of enhanced temperature control achieved through feedback with the power supply [11].

The global design requirements generally involve different and complex models, as they are subject to several physical phenomena: electromagnetic, thermal, structural, fluid dynamics... It is therefore interesting to address their study from a multiphysics perspective. In recent years, numerical simulation has emerged as an important tool for predicting the behavior of furnaces, since it allows changes to be made *in silico*, thus avoiding trial and error in the operation of the plant and in particular those relating to the feedback procedures with the power supply. This approach normally requires the use of modelling methodologies aimed at finding a compromise between accurate results and reasonable computation times. Although resistance furnaces are generally designed for a specific application, it is quite common to modify an existing furnace to operate in a different temperature range depending on the requirements. This can be done by adjusting the power supplied to the furnace, which in turn requires estimation of the input current. The need for fast models for control algorithms and real-time simulation is therefore important.

The prediction of the current distribution inside the resistance is a non-trivial matter, which can only be properly performed by numerical solution of the underlying electromagnetic models. This has already been done for other types of classical metallurgical furnaces (e.g.: induction furnaces [6, 28], arc furnaces [20, 30], or electron

beam furnaces [22, 26]). In contrast to all these technologies, the bibliography on mathematical modelling of industrial examples of indirect resistance furnaces is practically non-existent, which is a handicap when evaluating a new product.

In most cases, the heater has no cylindrical symmetry and, as a result, three-dimensional simulations are required, which are long and difficult. In addition, at the design stage, it is generally mandatory to know the response to different inputs, so a single simulation is not enough.

In this article, we present a methodology that requires a single numerical electromagnetic simulation to predict the response of the furnace to different current inputs. More specifically, we show how, from this initial numerical simulation, it is possible to obtain an equivalent lumped model for accurately estimating the current to be applied to the system in order to obtain the desired power.

The use of lumped models is something usual in industrial design (e.g., induction furnaces in [15, 18], electrochemical cells in [12] or power electronic converters in [16]). In our case, the novelty lies in the type of furnace and also in the fact that the proposed method can be applied to any resistance furnace powered by three-phase alternating current, whatever the geometry of the resistance and the rest of the elements that compose the device. In this context, it is worth mentioning that finding well-posed coupling between field problems and external circuits relies upon algebraic topology concepts as homology and cohomology spaces of the PDE domain, more specifically on Hodge theory (see [8, 13, 17, 23]). Moreover, building a discrete Hodge decomposition in the Whitney complex enables us to view the Galerkin finite element method as a way to set up circuit equations.

The paper is organized as follows: Section 2 presents the geometric configuration and the electromagnetic mathematical model of the furnace. Section 3 proposes an equivalent lumped model for analyzing the electrical behavior of the furnace. This model is based on the calculation of a reduced impedance associated with an equivalent circuit model. Section 4 presents numerical results from simulations performed on a real industrial furnace. The validity of the lumped model is demonstrated by comparing simulated and measured data. Section 5 discusses alternative methods for analyzing the furnace electrical circuits, highlighting their limitations compared to the original approach. The main conclusions are summarized in Section 6.

## 2 Statement of the problem

### 2.1 Geometry of the furnace

We consider a resistance furnace as the one depicted in Fig. 1. It consists of a stainless steel chamber that encloses a resistive heater and a workpiece placed over the heater. The workpiece consists of a hemispherical crucible containing the metal to be heated. Both the crucible and the resistance element are surrounded by air and insulating materials. Additionally, the chamber is equipped with an internal insulating lining, which helps to minimize heat losses.

The system is powered by a 3-phase alternating current (AC) for improved efficiency (in some applications, this ensures effective stirring of the load once it has been melted).

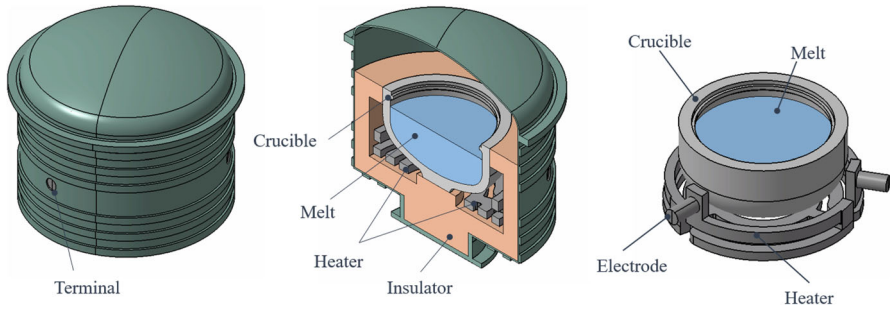


**Fig. 1** Furnace geometry. Isometric view (left), section (center), and detail (right)

The current is supplied to the resistance via three electrodes which pass through the chamber to the power supply circuit. Each of these electrodes receives an alternating current of the same amplitude but with different phases. These current parameters are the known input data for the system.

### 2.2 Mathematical model

In this section, we will present the three-dimensional mathematical model that allows us to calculate the current density distribution and the power dissipated in the different parts of the furnace and, in particular, in the resistance which is the goal of the study. For modelling purposes, we will introduce some notation. Let  $\Omega$  be a simply connected three-dimensional bounded domain consisting of two disjoint parts,  $\Omega_C$  and  $\Omega_D$ , representing conductors and dielectrics media, respectively. We will denote by  $\Omega_R$  the part of  $\Omega_C$  formed by the resistive heater and its terminals.

The computational domain  $\Omega$  is assumed to have a Lipschitz-continuous boundary denoted by  $\Gamma$ . Further, let  $\bar{\Gamma}_R := \partial\Omega_R \cap \Gamma$  be the outer boundary of  $\Omega_R$  and  $\bar{\Gamma}_D := \partial\Omega_D \cap \Gamma$  that of the dielectric domain. Finally,  $\mathbf{n}$  will represent any unit normal vector to a given surface. The computational domain is sketched in Fig. 2 according to the previous notations. Notice that  $\Gamma_R$  consists of three separate components denoted by

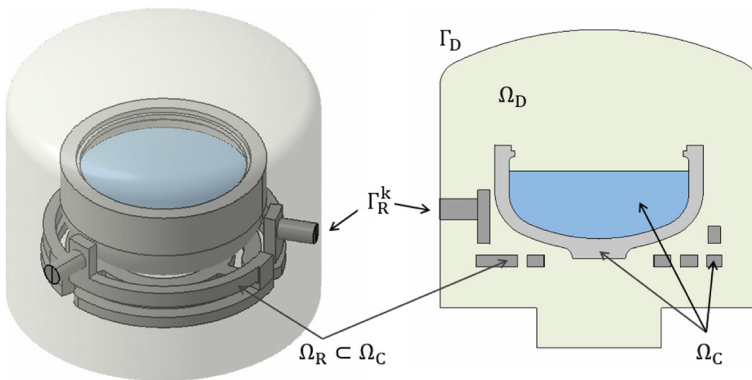


**Fig. 2** Computational domain and notations. Isometric (left) and section (right) views

$\Gamma_R^k, k = 1, \dots, 3$ , corresponding to the top of the electrodes where the current (or the voltage) will be prescribed.

The electromagnetic model is based on the well-known eddy current model and is solved numerically using a finite element method. Since the current source is alternating and all materials are assumed to have a linear electromagnetic behavior, we can use a time-harmonic approach. Thus, all of the fields involved in the Maxwell system have the form

$$\mathcal{F}(\mathbf{x}, t) = \text{Re}[\mathbf{F}(\mathbf{x})e^{i\omega t}], \tag{1}$$

where  $t$  is the time,  $\mathbf{x} \in \mathbb{R}^3$  is the space position,  $i$  is the imaginary unit,  $\mathbf{F}(\mathbf{x})$  is the complex amplitude (or phasor) of the field  $\mathcal{F}$  and  $\omega$  is the angular frequency,  $\omega = 2\pi f$ ,  $f$  being the frequency of the alternating current. For industrial cases with low and moderate frequencies, the quasi-static assumption applies and the term corresponding to the displacement current in the Ampere’s law can be neglected (a discussion of the parameter ranges in which this model is valid can be found in Bossavit’s work [8]). Furthermore, taking into account that the electric field is not required in non-conducting materials, the time-harmonic eddy current model leads to solve the following equations defined in  $\Omega$ :

$$\text{curl } \mathbf{H} = \mathbf{J}, \tag{2}$$

$$i\omega\mathbf{B} + \text{curl } \mathbf{E} = \mathbf{0}, \tag{3}$$

$$\text{div } \mathbf{B} = 0, \tag{4}$$

where  $\mathbf{H}, \mathbf{J}$ , and  $\mathbf{E}$  are the complex amplitudes associated with the magnetic field, the current density, and the electric field, respectively. For more details about these equations see, for instance, [7] or [25]. To obtain a closed system, we add the constitutive law  $\mathbf{B} = \mu\mathbf{H}$ , and the Ohm’s law  $\mathbf{J} = \sigma\mathbf{E}$ , where  $\mu$  is the magnetic permeability and  $\sigma$  is the electric conductivity, which is greater than zero in conductors and null in dielectrics.

The model must be completed with suitable boundary conditions, and we consider the following ones:

$$\mu\mathbf{H} \cdot \mathbf{n} = 0 \quad \text{on } \Gamma, \tag{5}$$

$$\mathbf{E} \times \mathbf{n} = \mathbf{0} \quad \text{on } \Gamma_R. \tag{6}$$

These boundary conditions were first proposed by Bossavit in [9]. The condition Eq. 5 implies that the magnetic field is tangential to the boundary of the chamber, while Eq. 6 means that the electric current enters the domain perpendicular to the cross section of the electrodes. Furthermore, Eq. 6 implies that the tangential component of the electric field  $\mathbf{E}$  is a gradient of a scalar potential  $V$  on the boundary of  $\Omega$ , and this potential must be constant on each connected component of  $\Gamma_R$  (see [5] for formal calculations). The sources are introduced into the model either by imposing a fixed potential drop between two connected components of  $\Gamma_R$  or by applying a fixed current across a connected component. In our case, the input current of the electrodes is assumed to be known. In particular, we will prescribe the current in two of the electrodes, i.e.,

$$\int_{\Gamma_R^k} \mathbf{J} \cdot \mathbf{n} dS = -I_k \quad k = 1, 2, \tag{7}$$

and on the third one, we will impose a null potential representing the ground

$$V_3 = 0 \quad \text{on } \Gamma_R^3. \tag{8}$$

The complex functions  $I_k = I_k e^{i\iota_k}$  in Eq. 7 are the phasors corresponding to the harmonic time-dependent signals  $\mathcal{I}_k(t) = I_k \cos(\omega t + \iota_k)$ ,  $k = 1, 2, 3$ , which are the real measurements at the terminals (see Fig. 3). Similarly, the complex functions  $V_k = V_k e^{i\epsilon_k}$  are the phasors corresponding to the signals  $\mathcal{V}_k(t) = V_k \cos(\omega t + \epsilon_k)$ ,  $k = 1, 2, 3$ .

This model, which takes into account in the boundary conditions the interfaces (ports) through which electromagnetic energy enters or leaves the system, is known in the literature as the *eddy current model with electric ports*. It can be handled by using different formulations [2, 7, 8]. In this work, we have considered the one based on the magnetic vector potential/scalar electric potential, namely, the well-known  $\mathbf{A}/V$  formulation. We recall here that the magnetic vector potential is derived from equation Eq. 4, which states the existence of a vector field  $\mathbf{A}$  such that  $\mathbf{B} = \mathbf{curl} \mathbf{A}$ . Conversely, the electric scalar potential  $V$  within the conducting domain is obtained from Faraday’s law,  $\mathbf{curl} (\mathbf{E} + i\omega \mathbf{A}) = \mathbf{0}$ , implying that  $\mathbf{E} + i\omega \mathbf{A} = -\mathbf{grad} V$ . The gauge condition  $\mathbf{div} \mathbf{A} = 0$ , along with appropriate boundary conditions, is imposed to ensure the uniqueness of the magnetic vector potential (see [3]).

Summarizing, the problem reads as follows:

Given complex numbers  $I_k$ ,  $k = 1, 2$ , find a vector field  $\mathbf{A}$  defined in  $\Omega$ , and a scalar field  $V$  defined in  $\Omega_C$  and constant in  $\Gamma_R^1, \Gamma_R^2$ , such that

$$\begin{aligned} \sigma(i\omega \mathbf{A} + \mathbf{grad} V) + \mathbf{curl} \left( \frac{1}{\mu} \mathbf{curl} \mathbf{A} \right) &= \mathbf{0} \text{ in } \Omega, \\ \mathbf{div} \mathbf{A} &= 0 \text{ in } \Omega, \\ \mathbf{A} \times \mathbf{n} &= 0 \text{ on } \Gamma, \\ \sigma(i\omega \mathbf{A} + \mathbf{grad} V) \cdot \mathbf{n} &= 0 \text{ on } \partial\Omega_C \setminus \Gamma_R, \\ V &= 0 \text{ on } \Gamma_R^3, \\ \int_{\Gamma_R^k} \sigma(i\omega \mathbf{A} + \mathbf{grad} V) \cdot \mathbf{n} \, dS &= -I_k, \quad k = 1, 2. \end{aligned}$$

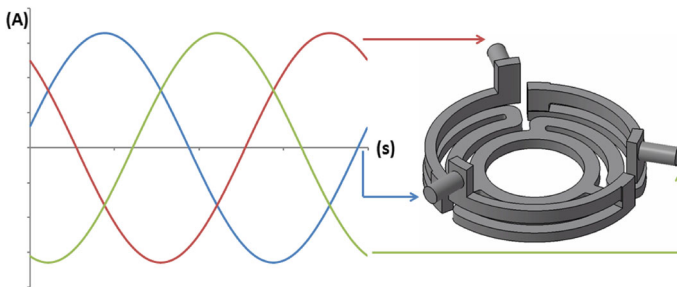


Fig. 3 Example of supplied intensity ( $\mathcal{I}_k(t)$ ,  $k = 1, 2, 3$ )

### 3 Equivalent lumped model

As mentioned earlier, the furnace is connected to an external electric circuit that provides the input currents to the electrodes. We assume that the heater has no external contacts other than these three terminals. We also assume that it is perfectly insulated inside the chamber and that there is no risk of leakage currents or ground faults. Under these assumptions, the circuit sketched in Fig. 4 applies.

The geometry of the resistance, as well as its location near the workpiece, causes different induction phenomena to occur. As a result, it is generally difficult to design an equivalent circuit for the entire furnace. However, if we combine all the passive elements of the circuit within the same block and forget about its particular topology, it is possible to replace it by a multi-terminal connected network as shown in Fig. 5, with six associated variables:  $\mathcal{I}_k, \mathcal{V}_k; k = 1, 2, 3$ .  $\mathcal{I}_k$  is the current that enters through the  $k$ -th terminal and  $\mathcal{V}_k$  is the potential of this terminal with respect to any potential reference. The terminal currents satisfy Kirchhoff’s current law, which states that the algebraic sum of the currents at any node of the network is zero, i.e.,

$$\sum_{k=1}^3 \mathcal{I}_k = 0. \tag{9}$$

According to the general theory of electrical multi-terminal networks, described in detail in the books of [4] and [10], and considering that the network has only passive elements, the currents can be expressed as a linear combination of the terminal voltages by means of the so-called *indefinite admittance matrix*. However, and as a consequence of Eq. 9, this is a singular matrix and, as it is shown in [19] or [29], it is not possible to obtain an impedance matrix to express the absolute voltages as a function of the currents.

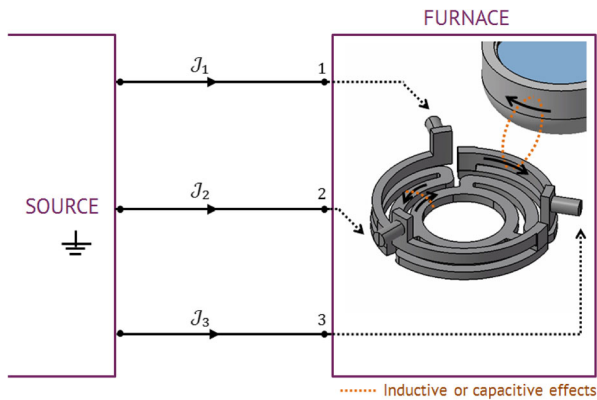


Fig. 4 Electrical three-phase supply via the furnace’s terminals

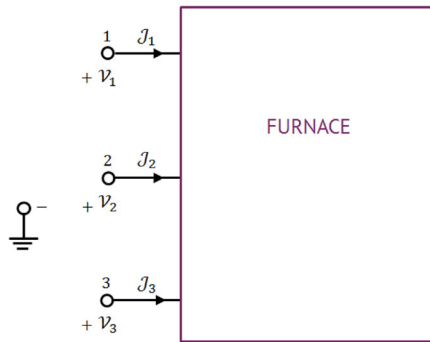


Fig. 5 Equivalent circuit

Furthermore, from Tellegen’s theorem [24], we deduce that the total power absorbed by the furnace network is the sum of the products  $V_k I_k$  at the three terminals. In particular, for alternating current [21], it holds

$$S = \frac{1}{2} \sum_{k=1}^3 V_k \bar{I}_k, \tag{10}$$

where  $S$  is the total complex power absorbed by the furnace and  $\bar{I}_k$  is the conjugate of  $I_k$ . The active power  $P$  (watts) is obtained from the real part of  $S$ . We note that  $P$  coincides with the active power  $P^h$  dissipated in the heater, which can be computed from the numerical simulation by using the usual formula

$$P^h = \int_{\Omega} \frac{|\mathbf{J}(\mathbf{x})|^2}{2\sigma} dV. \tag{11}$$

Thus, we can write

$$P^h = \text{Re}(S). \tag{12}$$

Then, for a given current data defined by two terminal currents  $I_1$  and  $I_2$ , we obtain the third one by applying Eq. 9, i.e.,  $I_3 = -I_2 - I_1$  and then complex power results

$$\begin{aligned} S &= \frac{1}{2} \sum_{k=1}^3 V_k \bar{I}_k \\ &= \frac{1}{2} ((V_1 - V_3) \bar{I}_1 + (V_2 - V_3) \bar{I}_2). \end{aligned}$$

Let us assume that the furnace operates with a balanced three-phase supply as the one shown in Fig. 3, with  $120^\circ$  phase shift between the electrodes,  $I_2 = I_1 e^{(2\pi/3)i}$ . Then, the complex power is

$$S = \frac{1}{2} ((V_1 - V_3) + (V_2 - V_3) e^{-(2\pi/3)i}) \bar{I}_1. \tag{13}$$



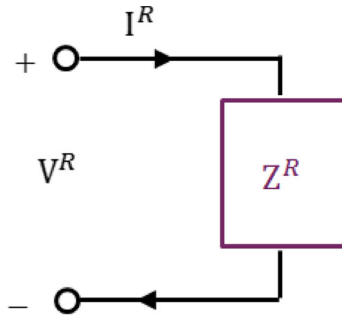


**Fig. 6** Reduced equivalent circuit

Equation 13 expresses the current supplied to one of the terminals as a function of the voltage drops between the terminals and the total power. We now define a reduced current and a reduced voltage drop as

$$I^R = I_1, \tag{14}$$

$$V^R = (V_1 - V_3) + (V_2 - V_3)e^{-(2\pi/3)i}. \tag{15}$$

As this network is linear and passive, the relation between  $I^R$  and  $V^R$  is constant. So we can define a reduced impedance as

$$Z^R = \frac{V^R}{I^R}, \tag{16}$$

and use the reduced model from Fig. 6 to study the furnace in terms of energy. In fact, the complex power corresponding to the impedance  $Z^R$  is the same as that obtained for the furnace in Eq. 13. For simplicity, let us denote  $|I^R| = I$ . Then, by replacing Eq. 16 in Eq. 13, we have

$$S = \frac{1}{2}Z^R I^2. \tag{17}$$

So, once we know the impedance value associated with the furnace, it is enough to know the amplitude of the terminal currents  $I$  to estimate the heat dissipated in the heater:




$$P^h = \frac{1}{2}\text{Re}(Z^R)I^2. \tag{18}$$

It is worth noting that the value of the reduced impedance can be computed by performing a single numerical simulation.

### 4 Numerical results and discussion

The numerical results presented in this section have been obtained using a real industrial furnace, the main geometrical characteristics of which are detailed in Tables 1 and 2, and in Fig. 7.

**Table 1** Material specifications in the furnace

Id	Color	Type	$\sigma$ ( $\Omega\text{m}$ )	$\mu_r$ (-)
Material 1		Conductor	$11.2\text{e}-6$	1
Material 2		Dielectric	—	—
Material 3		Conductor	$8.1\text{e}-7$	1

In the following, we will use the term ‘standard’ to refer to the operating conditions defined by  $|I_1| = I$ ,  $I_2 = Ie^{(2\pi/3)i}$  and  $I_3 = Ie^{-(2\pi/3)i}$ . The same operating conditions were applied to the furnace working in the plant in order to assess the numerical simulation and to calibrate all the parameters involved. From the numerical results, it is possible to compute and represent the Joule effect in the heater (Fig. 8) or the current density field (Figs. 9 and 10). As a post-processing result, we can also compute the output voltage at each terminal. The results are summarized in Table 3. Finally, the lumped model of the furnace is obtained by replacing the terminal voltages in Eq. 15. Thus, we obtain

$$V^R = V_1 + V_2e^{-(2\pi/3)i} = 64.3238 e^{-1.4172i} \text{ (V)}$$

**Table 2** Geometric data relating to Fig. 7

Id	Type	Dimension (mm or specified)
A <sub>1</sub>	Height	1380
A <sub>2</sub>	Height	980
A <sub>3</sub>	Height	400
B <sub>1</sub>	Diameter	1690
B <sub>2</sub>	Diameter	1380
B <sub>3</sub>	Height	350
C <sub>1</sub>	Arc	120°
C <sub>2</sub>	Diameter	1300
C <sub>3</sub>	Diameter	580
C <sub>4</sub>	Diameter	950
C <sub>5</sub>	Diameter	1100
C <sub>6</sub>	Height	29
C <sub>7</sub>	Height	215
C <sub>8</sub>	Height	150
C <sub>9</sub>	Height	65
C <sub>H</sub>	Height	2000
C <sub>R</sub>	Radius	475
C <sub>A</sub>	Area	0.7090 m <sup>2</sup>
C <sub>V</sub>	Volume	0.1999 m <sup>3</sup>

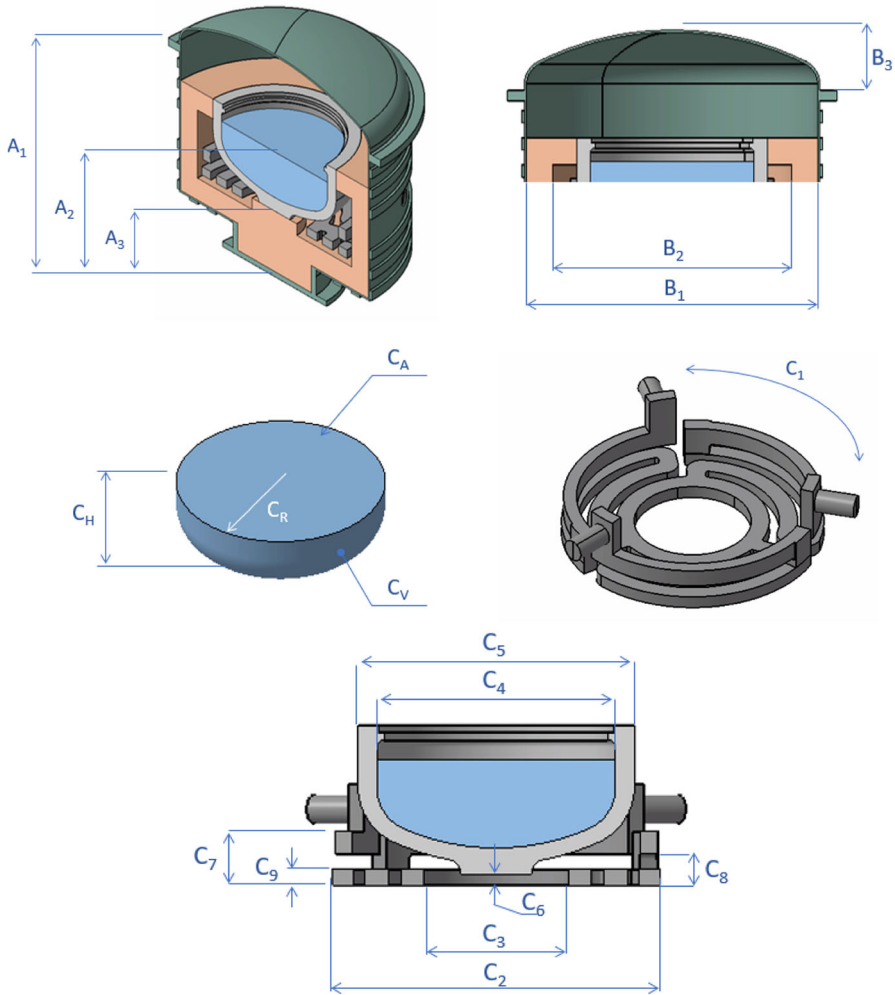
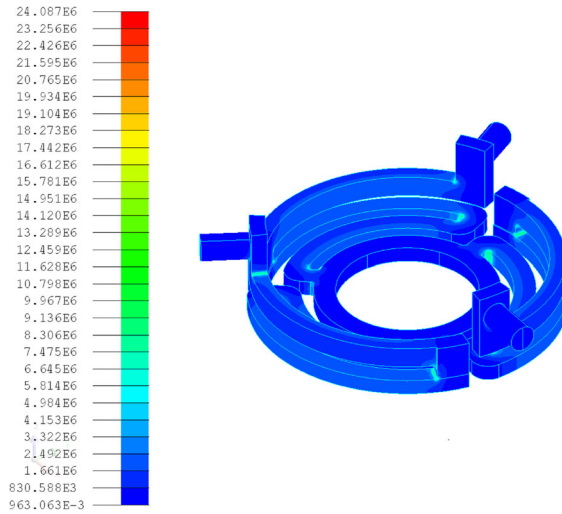


Fig. 7 Data related to different parts within the furnace geometry, as specified in Table 2

and then

$$Z^R = \frac{V^R}{I^R} = 0.2063 e^{-3.0975i}$$

Now, the thermal dissipation in the heater can be adjusted to operate under conditions other than the standard ones through a simple procedure. Indeed, once the value of  $Z^R$  is obtained, the input current required to achieve the target power is immediately determined using Eq. 18. Thus, a characteristic curve representing the power dissipation as a function of the current amplitude can be generated, as the solid line in Fig. 11. To validate the accuracy of this curve, the currents measured in-plant corresponding to other desired power dissipation levels (110, 120, and 160 kW) have been added to the



**Fig. 8** Joule losses on the furnace heater under standard conditions ( $\text{W/m}^3$ )

graph. To facilitate comparison, the corresponding values obtained directly from the reduced lumped model have also been highlighted alongside the measured values in the plant. As shown in Table 4, the errors are all less than 3%. In addition, the currents and voltages obtained from the corresponding numerical simulations are summarized in Table 5.

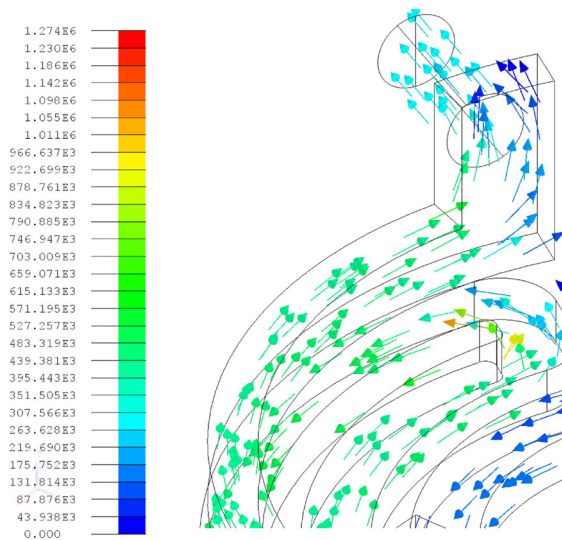


**Fig. 9** Current density vector in the neighborhood of a terminal

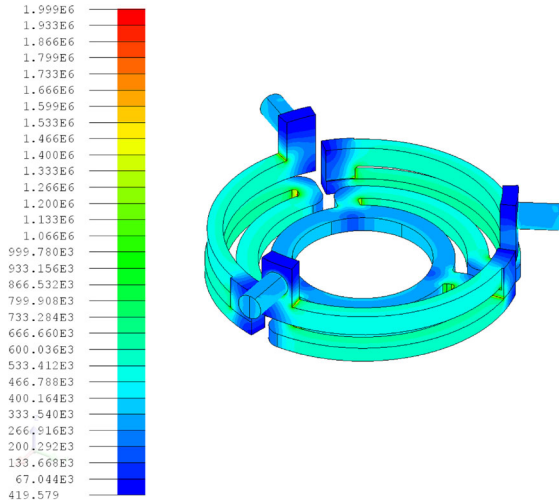


Fig. 10 Modulus of the current density ( $A/m^2$ )

Table 3 Terminal voltages ( $V$ , rad) and dissipated power (kW) for the standard operating conditions of current supplied (A)

$ IR $	$(V_1, \epsilon_1)$	$(V_2, \epsilon_2)$	$(V_3, \epsilon_3)$	$P^h(\Omega)$
3116.79	(37.14, -0.89)	(37.13, 0.15)	(0, 0)	100.15

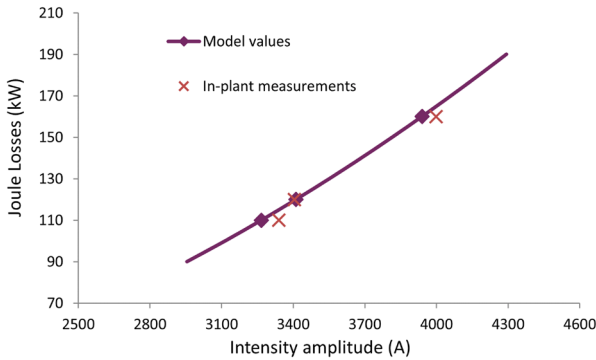


Fig. 11 Characteristic curve of the furnace representing the power dissipation in the heater as a function of the current amplitude. Markers show the comparison between plant-measured and lumped model-calculated values

Table 4 Current (A) measured in plant and from the model computations

Power (kW)	In-plant measures	Model results	Relative error (%)
160	3998	3939	1.48
120	3405	3411	0.18
110	3339	3267	2.16

**Table 5** Terminal voltages (V, rad) and dissipated power (kW) as a function of current supplied (A)

$ I^R $	3266.55	3411.80	3939.61
$(V_1, \epsilon_1)$	(38.92, $-0.89$ )	(40.65, $-0.89$ )	(46.94, $-0.89$ )
$(V_2, \epsilon_2)$	(38.92, 0.15)	(40.66, 0.15)	(46.94, 0.15)
$(V_3, \epsilon_3)$	(0, 0)	(0, 0)	(0, 0)
$P^h(\Omega)$	109.98	119.98	159.97

## 5 Some remarks

### 5.1 Reduced impedance method versus heater equivalent circuit

As an alternative to the reduced impedance method described in Section 3, one could consider replacing the furnace resistance with an equivalent electrical circuit (see Fig. 12). This has two main drawbacks. The first one is that the geometry of the resistance should be simple enough to do the calculation by hand. Note that this would not be necessary when using the reduced impedance method. In fact, to use this method, one should only make measurements at the terminals of the furnace to know its voltages. This would not be possible at the design stage, but it is very easy when the furnace is already operating in the plant. On the other hand, this equivalent electrical circuit would not take into account possible induction phenomena between the furnace parts. Although in the example shown in this paper this phenomenon has little influence on the impedance calculation (it is almost 100% resistive), this may not be the case when considering other types of furnaces operating at higher frequencies, such as, for instance, induction furnaces. However, the methodology based on the reduced impedance could also be easily adapted to this case: in the first step, an initial numerical simulation has to be done, and then, in the second step and from the results of the numerical simulation, the reduced impedance can be calculated.

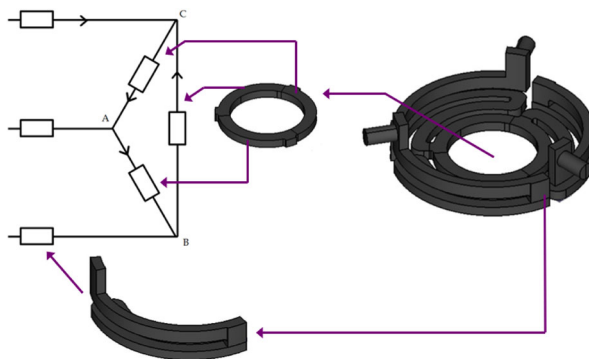


**Fig. 12** Heater equivalent circuit construction

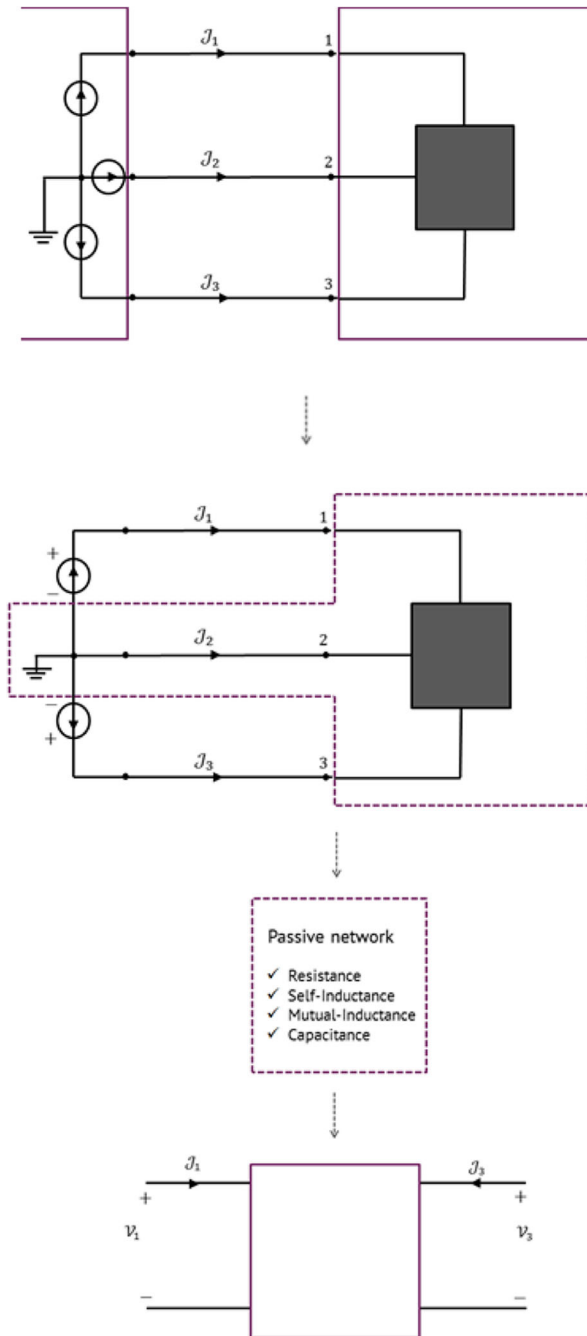


Fig. 13 Transforming a multi-terminal network into a two-port network

## 5.2 Multi-terminal network versus two-port network

Let us remember that the electric current is supplied to the furnace through 3 electrodes that go from the resistance to the power supply traversing the furnace housing. In general, this current is the only data, and neither the internal geometry of the furnace nor the “upstream” circuit associated with the current supply is known. As explained in previous sections, a voltage with respect to a random reference is associated with each of the 3 terminals, so that the equivalent circuit is a multi-terminal network like the one shown in Fig. 5. Remember also that the reduced impedance method proposed in this paper is derived starting from this multi-terminal network. For this type of circuit, it is possible to write an intensity-voltage relationship in terms of the admittance matrix such that  $[I] = [Y][V]$ . Since  $[Y]$  is a singular matrix, it is not possible to express the absolute potentials of each terminal as a function of the currents. Nevertheless, it would be possible to compute an impedance matrix for this multi-terminal network, but first, it must be transformed into a two-port network (see Fig. 13). This involves making a number of simplifications and assumptions about the “upstream” source circuit, which results in a certain loss of generality. In particular, the impedance and/or admittance matrices only make sense if any nonlinearity is discarded. This restriction does not occur in the reduced impedance method explained above, since only Tellegen’s theorem and Kirchhoff’s laws are used, and therefore the two-port network option is not considered here.

## 6 Conclusions

This paper presents a method combining a distributed and a lumped model to determine the electromagnetic behavior of a three-phase indirect resistance furnace. The method proves to be particularly useful at the design stage of the installation. From an initial single numerical simulation (taking into account induction phenomena), a reduced impedance associated with the furnace is computed. From this value, it is possible to construct a curve relating the intensity supplied to the thermal power dissipated by the furnace, without having to carry out further numerical simulations and avoiding long and costly trial-and-error procedures in the plant. Moreover, the method is general in the sense that it is independent both of the upstream circuit and of the topology and materials that may be present inside the furnace. Some numerical results for a real industrial furnace are shown that assess the performance of the proposed methodology.

**Acknowledgements** The authors acknowledge and appreciate the impact that Alain Bossavit’s work has had on their research related to the mathematical analysis of numerical methods to solve electromagnetism problems and to the application to the mathematical modeling of various industrial problems.

**Funding** Open Access funding provided thanks to the CRUE-CSIC agreement with Springer Nature. This work has been partially supported by FEDER, Ministerio de Ciencia e Innovación through the research project PID2021-122625OB-I00 and by Xunta de Galicia (Spain) research project GI-1563 ED431C 2021/15.



## Declarations

**Conflict of interest** The authors declare no competing interests.

**Open Access** This article is licensed under a Creative Commons Attribution 4.0 International License, which permits use, sharing, adaptation, distribution and reproduction in any medium or format, as long as you give appropriate credit to the original author(s) and the source, provide a link to the Creative Commons licence, and indicate if changes were made. The images or other third party material in this article are included in the article's Creative Commons licence, unless indicated otherwise in a credit line to the material. If material is not included in the article's Creative Commons licence and your intended use is not permitted by statutory regulation or exceeds the permitted use, you will need to obtain permission directly from the copyright holder. To view a copy of this licence, visit <http://creativecommons.org/licenses/by/4.0/>.

## References

1. Adachi, M., Yonemori, H.: Considerations of configurations on induction heating type indirect heating system. In: Proceedings of the IEEE region 10 humanitarian technology conference 2014, vol. 2015–Jan, pp. 88–93 (2015)
2. Alonso-Rodríguez, A., Valli, A.: Eddy current approximation of Maxwell equations: theory. Algorithms and Applications. Springer, Milan (2010)
3. Amrouche, C., Bernardi, C., Dauge, M., Girault, V.: Vector potentials in three-dimensional non-smooth domains. *Math. Methods Appl. Sci.* **21**(9), 823–864 (1998)
4. Balabanian, N., Bickart, T.: Electrical network theory. Wiley, New York (1969)
5. Bermúdez, A., Rodríguez R., Salgado, P.: Numerical solution of eddy current problems in bounded domains using realistic boundary conditions. *Comput. Methods Appl. Mech. Eng.* **194**(2), 411–426 (2005)
6. Bermúdez, A., Gómez, D., Muñoz, M.C., Salgado, P.: Transient numerical simulation of a thermoelectrical problem in cylindrical induction heating furnaces. *Adv. Comput. Math.* **26**(1–3), 39–62 (2007)
7. Bermúdez, A., Gómez, D., Salgado, P.: Mathematical models and numerical simulation in electromagnetism. Springer, New York (2014)
8. Bossavit, A.: Computational electromagnetism: variational formulations, complementarity. Edge Elements. Academic Press series in electromagnetism. Academic Press, San Diego, CA (1998)
9. Bossavit, A.: Most general “non-local” boundary conditions for the Maxwell equation in a bounded region. *COMPTEL - Int. J. Comput. Math. Electr. Electron. Eng.* **19**(2), 239–245 (2000)
10. Callegaro, L.: Electrical impedance. Measurements and Applications. Taylor & Francis, Boca Raton, Principles (2013)
11. Edgerley, C., Smith, L., Wilford, C.F.: Electric metal melting - a review. *Power Eng. J.* **2**(2), 83–92 (1988)
12. Fletcher, S.: The two-terminal equivalent network of a three-terminal electrochemical cell. *Electrochem. Commun.* **3**, 692–696 (2001)
13. Gross, P.W., Kotiuga, P.R.: Electromagnetic theory and computation: a topological approach, 1st edn. No. 48 in Mathematical Sciences Research Institute Publications. Cambridge University Press, Cambridge (2004)
14. Grzella, J., Sturm, P., Krüger, J., Reuter, M.A., Kögler, C., Probst, T.: Metallurgical furnaces. In: Ullmann's Encyclopedia of Industrial Chemistry. Wiley-VCH Verlag GmbH & Co. KGaA (2003)
15. Jankowski, T.A., Pawley, N.H., Gonzales, L.M., Ross, C.A., Jurney, J.D.: Approximate analytical solution for induction heating of solid cylinders. *Appl. Math. Model.* **40**(4), 2770–2782 (2016)
16. Kawashima, R., Mishima, T., Ide, C.: Three-phase to single-phase multiresonant direct AC-AC converter for metal hardening high-frequency induction heating applications. *IEEE Trans. Power Electron.* **36**(1), 639–653 (2021)
17. Kettunen, L.: Fields and circuits in computational electromagnetism. *IEEE Trans. Magn.* **37**(5), 3393–3396 (2001)

18. Nguyen, B.A., Phan, Q.D., Nguyen, D.M., Nguyen, K.L., Durrieu, O., Maussion, P.: Parameter identification method for a three-phase induction heating system. *IEEE Trans. Ind. Appl.* **51**(6), 4853–4860 (2015)
19. Puckett, T.: A note on the admittance and impedance matrices of a n-terminal network. *IRE Transactions - Circuit Theory* **CT-3**, 70–75 (1956)
20. Ramírez, M., Trapaga, G.: Mathematical modeling of a direct current electric arc: part I. Analysis of the characteristics of a direct current arc. *Metallurgical and Materials Transactions B: Process Metallurgy and Materials Processing Science* **35**(2), 363–372 (2004)
21. Redondo, R.C., Melchor, N.R., Redondo, M., Quintela, F.R.: Electrical power and energy systems instantaneous active and reactive powers in electrical network theory: a review of some properties. *Int. J. Electr. Power Energy Syst.* **53**, 548–552 (2013)
22. Tan, Y., Wen, S., Shi, S., Jiang, D., Dong, W., Guo, X.: Numerical simulation for parameter optimization of silicon purification by electron beam melting. *Vacuum* **95**, 18–24 (2013)
23. Tarhasaari, T., Kettunen, L., Bossavit, A.: Some realizations of a discrete Hodge operator: a reinterpretation of finite element techniques [for EM field analysis]. *IEEE Trans. Magn.* **35**(3), 1494–1497 (1999)
24. Tellegen, B.: A general network theorem, with applications. *Philips Res. Rep.* **7**, 259–269 (1952)
25. Touzani, R., Rappaz, J.: *Mathematical models for eddy currents and magnetostatics*. Scientific Computation. Springer, Dordrecht (2014)
26. Vutova, K., Donchev, V.: Non-stationary heat model for electron beam melting and refining - an economic and conservative numerical method. *Appl. Math. Model.* **40**(2), 1565–1575 (2016)
27. Walton, R.R.: *Furnaces, electric, resistance furnaces*, p. 12. Wiley, Ltd, New Jersey (2000)
28. Yermekova, M., Galunin, S.A.: Numerical simulation and automatic optimization of the disk induction heating system. In: *Proceedings of the 2017 IEEE Russia section young researchers in electrical and electronic engineering conference, ElConRus 2017*, pp. 1085–1090 (2017)
29. Zadeh, L.A.: Multipole analysis of active networks. *IRE Trans. Circ. Theory* **4**(3), 97–105 (1957)
30. Zhang, X.K., He, Y.L., Tang, S.Z., Wang, F.L., Xie, T.: An electromagnetics-temperature-component multi-physical coupled model for electric furnace in calcium carbide smelting process. *Appl. Therm. Eng.* **165**, 114552 (2020)

**Publisher's Note** Springer Nature remains neutral with regard to jurisdictional claims in published maps and institutional affiliations.